THE ASTROPHYSICAL JOURNAL

AN INTERNATIONAL REVIEW OF SPECTROSCOPY AND ASTRONOMICAL PHYSICS

VOLUME 87 MARCH 1938 NUMBER 2

EQUIVALENT WIDTHS AND THE TEMPERATURE OF THE SOLAR REVERSING LAYER

DONALD H. MENZEL, JAMES G. BAKER, AND LEO GOLDBERG

ABSTRACT

Allen's extensive determinations of equivalent widths of Fraunhofer lines provide important observational material for an analysis of the physical state of the solar atmosphere. A comparison of the observed intensities of absorption lines, as read from an empirical curve of growth, with the theoretical strengths of lines in a transition array makes it possible to calculate the effective excitation temperature of the reversing layer. Temperatures of 4350° ± 200° and 4150° ± 50° are computed from the lines of *Ti* I and *Fe* I, respectively.

A qualitative discussion of the errors inherent in the theoretical calculation of multiplet strengths is given, and a method for calculating the reversing-layer temperature by means of the *J*-file sum rule is described. The application of this method to the lines of *Ti* I yields a temperature of 4400° ± 100°. Since the sum rule is independent of the coupling in an atom, and is therefore free of the assumptions involved in the calculation of multiplet strengths, the value 4400° is adopted, for purposes of discussion, as the mean excitation temperature of the solar reversing layer.

If the opacity of the solar atmosphere varies with wave length, we should expect to find the numbers of atoms, as derived from equivalent widths, depending upon wave length as well as upon the temperature and excitation potential. The data for *Fe* indicate an opacity law almost independent of wave length. These results, however, are not definitive. Since the mean lower excitation potentials increase systematically with wave length, opacity and temperature effects are correlated. The data for *Ti*, where no systematic correlation exists, are not inconsistent with an opacity varying as λ^3, whereas theory predicts a law varying approximately as $\lambda^3 e^{-hc/\lambda kT}$. An attempt is made to reconcile the observations and the theoretical values.

The observed intensities of the Fraunhofer lines may be employed in an analysis of the physical state of the solar atmosphere. The functional relationship between the equivalent widths, W, of the solar lines, and the theoretical strengths of the atomic transitions

has been developed by Minnaert and Slob[1] and by Menzel.[2] In this paper we shall combine theory with observational data in an attempt to determine the effective excitation temperature of the solar reversing layer. Baker[3] has derived the following semi-empirical formula that relates W/λ to various atomic and physical parameters:

$$\log \frac{W}{\lambda} = \log X_0 \frac{v}{c}\sqrt{\pi} - \tfrac{1}{2}\log(1 + X_0) - \frac{\tfrac{1}{2}\log 4\sqrt{\pi}\,\frac{v}{c}\,\frac{\nu}{\Gamma}}{1 + 15e^{-2\log X_0}}, \qquad (1)$$

where[4]

$$\left.\begin{aligned} X_0 &= \frac{N_a}{b(T)}\, e^{-\chi_{J'}/kT}\, \frac{1}{3\sqrt{\pi}R}\, \frac{\pi e^2}{mc}\, \phi\, \frac{c}{v}\, S\, \frac{s}{\Sigma s} \\ &= \left[3.510 \times 10^{-12}\, \frac{N_a}{b(T)}\, \sqrt{\frac{\mu}{T}}\, \phi\right] S\, \frac{s}{\Sigma s}\, e^{-\chi_{J'}/kT}. \end{aligned}\right\} \qquad (2)$$

Physically, X_0 is equal to the optical depth at the center of the absorption line.

The factor in brackets is constant for all the lines of a transition array. For lines of the same multiplet, the $\chi_{J'}$'s are essentially equal, and X_0 depends only on $s/\Sigma s$. Equation (1) defines the curve of growth as a function of X_0, and hence for a multiplet the curve is a function of $s/\Sigma s$. Furthermore, the curves of growth for different multiplets will all have the same shape, as long as Γ/ν and v are the same. They may be brought into coincidence by a horizontal shift along the X_0 axis. This is the customary procedure for determining the curve of growth. Allen,[5] who utilized his own observational data for the determination, found that W/λ, rather than W, must be employed for the ordinate if lines in different wave-length

[1] *Proc. Amsterdam Acad.*, **34**, Part 1, 542, 1931.

[2] *Ap. J.*, **84**, 462, 1936. A preliminary report of the results of the present investigation appeared in *Pub. A.A.S.*, **8**, 218, 1936.

[3] *Ap. J.*, **84**, 474, 1936. A list of definitions of the various algebraic quantities occurring in the foregoing discussion appears at the end of this paper.

[4] Menzel, *loc. cit.*

[5] *Mem. Comm. Solar Obs.*, **1**, No. 5, 1934.

regions are to be combined on the same diagram. This procedure, by equation (1), is seen to be justified theoretically.[6]

In proceeding to determine the effective excitation temperature of the solar reversing layer, our first act was to rederive the curve of growth from Allen's extensive tabulation of equivalent widths and from the theoretical strengths of multiplet lines. The observational data were tabulated by multiplets, and the quantity $\log W/\lambda$ was computed for each line directly from the tabular values. For each line of a multiplet, $\log W/\lambda$ was plotted against $\log s/\Sigma s$. The

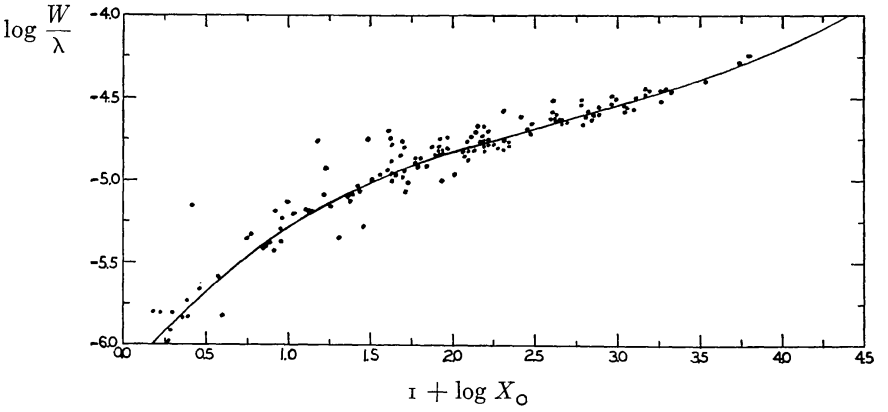

FIG. 1

ten best-determined curves were combined to give a mean curve of growth. The remaining diagrams were then superposed on the master-curve, and the observational points were transferred. The final curve that was drawn through all of these points is reproduced in Figure 1. The observational scatter is small. That the few widely divergent points represent blends is evident, since most of the discrepant points lie *above* the determined curve of growth. The curve agrees substantially with that given by Allen.

The next procedure was to fit the observed curve to the theoretical formula (1). A value of v, corresponding to *Fe* atoms at a temperature of 5740°, was found to fit the observations satisfactorily in the lower part of the curve, and the value of $1.52 \cdot 10^{-6}$ was derived for Γ/ν from the damping portion of the curve.

[6] Menzel, *loc. cit.*

For a given observed value of log W/λ we were able to read off the value of log X_0 from Figure 1. Now, by (2), for each transition array,

$$\log X_0 = L + \log S - \log \frac{\Sigma s}{s} - \frac{5040}{T} \chi_{J'}, \tag{3}$$

where L is equal to

$$\log \left[3.510 \times 10^{-12} \frac{N_a}{b(T)} \sqrt{\frac{\mu}{T}} \phi \right]. \tag{4}$$

If we set

$$\log X_0' = \log S - \log \frac{\Sigma s}{s}, \tag{5}$$

we have

$$Y = \log X_0 - \log X_0' = L - \frac{5040}{T} \chi_{J'}. \tag{6}$$

Y is defined by the foregoing equation.

Log X_0' was computed for each line from equation (5). Values of log $s/\Sigma s$ have been tabulated by Russell.[7] Goldberg[8] has computed values of S, the relative multiplet strengths. The applicability of these theoretical calculations may be questioned on the grounds that complex atoms clearly deviate from LS coupling and are strongly affected by configuration overlapping, but no better values of log X_0' are available. Eventually, when more precise determinations are at hand, either from theoretical calculations or from experiment,[9] the present analysis should be repeated. Further discussion of the effects of configuration interaction and of departures from LS coupling will be found later on in this paper.

For each line of an array we obtain a value of Y. For the present we shall assume that N_a is independent of λ, which is equivalent to ignoring the variation of opacity with wave length. Then (6) is the equation of a straight line of slope $-5040/T$ and intercept L. If, for each transition array, we plot the determined values of Y against the corresponding lower excitation potentials, the slope of the resulting straight line affords a determination of the effective excitation temperature T. A total of fourteen transition arrays, including over four hundred lines, was investigated. Table 1 contains the observa-

[7] *Ap. J.*, **83**, 129, 1936.

[8] *Ibid.*, **82**, 1, 1935.

[9] R. B. King and A. S. King, *ibid.*, p. 377.

TABLE 1

Multiplet	S	$\bar{\lambda}$	$\overline{\log X_0'}$	$\bar{Y}$	$\bar{x}_{J'}$	No. of Lines
			Ca I, 4s4p—4s4d			
$4^3P^o-4^3D$.....	3	4444	−0.57	3.69	1.883	6
$4^1P^o-4^1D$.....	1	7326	0.00	1.88	2.920	1
			Ca I, 4s4p—4p²			
$4^3P^o-p^2\,{}^3P$.....	9	4300	0.10	3.20	1.881	6
$4^1P^o-p^2\,{}^1D$.....	5	5857	0.70	2.00	2.920	1
$4^1P^o-p^2\,{}^1S$.....	1	5868	0.00	0.77	2.920	1
			Ca I, 4s4p—4s6s			
$4^1P^o-6^1S$.....	1	5513	0.00	2.00	2.920	1
			Ca I, 4s4p—4s6d			
$4^1P^o-6^1D$.....	1	4685	0.00	1.54	2.920	1
			Ca I, 4s4p—4s7s			
$4^1P^o-7^1S$.....	1	4847	0.00	0.88	2.920	1
			Ca I, 4s3d—4s5p			
$3^1D-5^1P^o$.....	1	5042	0.00	2.20	2.697	1
$3^3D-5^3P^o$.....	3	6164	−0.33	2.09	2.512	5
			Ca I, 3d4s—3d4p			
$3^3D-dp^3P^o$.....	9	5264	−0.09	2.29	2.511	5
$3^1D-dp^1F^o$.....	7	5349	0.85	1.45	2.697	1
$3^3D-dp^3D^o$.....	15	5593	0.23	2.36	2.512	6
$3^3D-dp^3F^o$.....	21	6479	0.07	2.03	2.513	6
$3^1D-dp^1P^o$.....	3	6718	0.48	1.74	2.697	1
$3^1D-dp^1D^o$.....	5	7148	0.70	1.64	2.697	1

TABLE 1—*Continued*

Multiplet	S	$\bar{\lambda}$	$\overline{\log X'_0}$	$\bar{Y}$	$\bar{X}_{J'}$	No. of Lines
			Ca I, 4s3d—4s6p			
$3^3D-6^3P^o$	3	4510	0.02	0.72	2.514	2
$3^1D-6^1P^o$	1	4527	0.00	2.20	2.697	1
			Ti I, $3d^24s4p-3d^24s5s$			
$z^5G^o-e^5F$	45	4988	0.59	0.72	1.980	8
$z^5F^o-e^5F$	35	5225	0.36	0.28	2.095	10
$z^5D^o-e^5F$	25	5705	0.44	−0.01	2.290	6
			Ti I, $3d^34s-3d^24s4p$			
$a^1H-x^1H^o$	792	4278	2.90	−0.87	2.567	1
$a^5F-y^5D^o$	2520	5240	2.37	−2.17	0.827	4
$a^3G-v^3F^o$	648	5270	1.78	−1.18	1.875	2
$a^1H-x^1G^o$	1188	5504	3.08	−2.49	2.567	1
$a^3G-z^3H^o$	264	5980	1.93	−1.14	1.872	3
			Ti I, $3d^34s-3d^34p$			
$a^5F-x^5D^o$	25	4290	0.20	2.06	0.821	10
$a^5P-y^5S^o$	5	4285	0.22	1.62	1.732	1
$a^3H-u^3G^o$	27	4322	0.84	0.24	2.227	1
$a^3D-v^3P^o$	9	4354	0.62	0.71	2.165	1
$b^3P-r^3D^o$	15	4420	0.72	0.21	2.235	2
$a^3G-v^3G^o$	27	4450	0.18	0.76	1.872	6
$a^5P-y^5P^o$	15	4480	0.24	1.13	1.733	7
$a^5F-y^5F^o$	35	4535	0.30	1.97	0.824	13
$c^3P-x^3S^o$	3	4558	0.22	0.71	2.335	1
$a^5P-w^5D^o$	25	4640	0.28	0.91	1.734	8
$a^3H-x^3H^o$	33	4752	0.65	0.36	2.234	4
$c^3P-s^3D^o$	15	4803	0.55	0.53	2.33	3
$a^3H-z^3I^o$	39	4874	0.71	0.22	2.235	4
$a^3G-y^3H^o$	33	4908	0.47	0.52	1.873	5
$a^3D-u^3F^o$	21	4932	0.79	0.21	2.153	3
$b^1D-w^1F^o$	7	4975	0.85	−0.37	2.495	1
$a^5F-y^5G^o$	45	5017	0.08	1.73	0.838	12
$a^1H-z^1I^o$	13	5120	1.11	−0.14	2.567	1
$c^3P-w^3P^o$	9	5455	0.57	−0.19	2.335	1
$b^3F-w^3D^o$	15	5500	0.29	0.49	1.435	5
$b^1G-y^1G^o$	9	5644	0.95	−0.11	2.258	1
$b^1G-z^1H^o$	11	6091	1.04	−0.57	2.258	1
$b^3F-y^3G^o$	27	6280	0.63	0.37	1.442	4
$b^3F-x^3F^o$	21	6540	0.84	−0.39	1.445	2

TABLE 1—*Continued*

Multiplet	S	$\bar{\lambda}$	$\overline{\log X'_0}$	$\bar{Y}$	$\bar{X}_{J'}$	No. of Lines
	Ti I, $3d^24s4p-3d^24s4d$					
$z^1G^o-e^1H$	1320	4809	3.12	0.63	3.049	1
	Ti II, $3d^3-3d^24p$					
$a^4P-z^4D^o$	336	4310	1.38	1.28	1.165	7
$a^2G-z^2F^o$	337.5	4471	1.72	0.88	1.116	3
$a^2H-z^2G^o$	660	4550	1.95	0.89	1.569	3
$a^2P-z^2D^o$	9	4563	1.35	1.36	1.227	3
$b^2F-y^2G^o$	112.5	4377	1.68	−0.07	2.582	1
$b^2D-z^2D^o$	156.7	5208	1.50	0.52	1.564	3
	V I, $3d^44s-3d^44p$					
$a^6D-y^6D^o$	15	4115	0.09	2.09	0.278	8
$a^6D-y^6F^o$	21	4405	−0.12	2.07	0.280	11
$a^4H-z^4I^o$	26	4470	0.44	0.60	1.852	4
$a^4D-y^4D^o$	10	5625	0.15	0.36	1.076	2
$a^4D-y^4F^o$	14	5730	0.24	0.45	1.057	5
$a^4D-y^4P^o$	6	6080	−0.06	0.63	1.056	5
	Cr I, $3d^44s4p-3d^44s5s$					
$z^7D^o-f^7D$	35	5220	0.35	0.38	3.398	8
$y^5P^o-e^5D$	15	5240	0.45	−0.28	3.652	1
$z^7F^o-f^7D$	49	4670	0.31	0.82	3.118	14
$y^7P^o-f^7D$	21	5300	−1.14	1.72	3.434	8
$z^5F^o-e^5D$	35	5650	0.74	−0.16	3.831	3
$z^5D^o-e^5D$	25	6630	0.37	0.20	4.157	2
	Cr I, $3d^54s-3d^54p$					
$a^7S-z^7P^o$	7	4270	1.37	3.72	0.000	2
$a^5S-z^5P^o$	5	5206	1.52	3.32	0.937	3
	Mn I, $3d^64s-3d^64p$					
$a^6D-z^6D^o$	15	4050	0.03	2.76	2.152	9
$a^4D-y^4P^o$	6	4250	−0.22	2.05	2.918	7
$a^4D-z^4D^o$	10	4450	−0.10	1.96	2.914	10
$a^4D-z^4F^o$	14	4700	−0.04	1.90	2.904	7

TABLE 1—*Continued*

Multiplet	S	$\bar{\lambda}$	$\overline{\log X_0'}$	$\bar{Y}$	$\bar{X}_{J'}$	No. of Lines
	Mn I, $3d^5 4s4p - 3d^5 4s5s$					
$z^8P^o - e^8S$	4	4800	0.14	2.91	2.290	3
$z^4P^o - e^4S$	2	5400	−0.22	1.13	3.835	3
$z^6P^o - e^6S$	3	6000	−0.01	1.96	3.060	3
	Mn I, $3d^5 4s4p - 3d^5 4s4d$					
$z^6P^o - e^6D$	3	4450	−0.52	2.64	3.060	8
	Fe I, $3d^7 4s - 3d^7 4p$					
$a^3F - y^3F^o$	21	4091	0.37	4.65	1.556	5
$b^3P - z^3S^o$	3	4062	−0.08	3.21	2.833	3
$a^3F - z^3G^o$	27	4251	0.05	4.49	1.523	6
$a^5P - z^5S^o$	5	4317	0.20	3.20	2.189	3
	Fe I, $3d^6 4s4p - 3d^6 4s5s$					
$z^7D^o - e^7D$	35	4225	0.40	3.86	2.439	10
$z^7F^o - e^7D$	49	4926	0.20	3.34	2.851	12
$z^3D^o - e^3D$	15	4970	0.22	1.92	3.907	6
$z^3F^o - e^3D$	21	5053	0.43	1.98	3.940	5
$z^7P^o - e^7D$	21	5193	0.31	3.25	2.979	9
$z^5D^o - e^5D$	25	5275	0.20	2.81	3.243	12
$z^3P^o - e^3D$	9	5672	0.14	1.84	4.220	6
$z^5F^o - e^5D$	35	5644	0.14	2.53	3.386	9
$y^5P^o - f^5D$	15	6766	0.15	1.23	4.593	7
	Ni I, $3d^9 4p - 3d^9 4d$					
$z^3P^o - f^3D$	63	4800	0.98	0.72	3.599	5
$z^3F^o - e^3F$	84	4295	1.30	0.59	3.700	2
$z^3F^o - e^3G$	324	4970	2.01	0.71	3.680	3
$z^3D^o - e^3F$	168	5010	1.47	0.42	3.698	4
$z^3D^o - f^3D$	105	5180	1.41	0.53	3.721	3
$z^3P^o - e^3P$	81	4900	1.09	0.67	3.642	4
$z^3P^o - e^3S$	36	5120	1.30	1.15	3.527	1
$z^3F^o - f^3D$	12	5020	0.11	1.53	3.626	2
$z^1F^o - e^1F$	28	5049	1.45	0.44	3.831	1
$z^1F^o - e^1G$	108	5081	2.03	0.53	3.831	1
$z^3D^o - e^3P$	27	5160	0.96	0.79	3.676	2
$z^1D^o - e^1F$	56	5156	1.75	0.41	3.881	1
$z^1D^o - f^1D$	35	5177	1.54	0.14	3.881	1
$z^1P^o - e^1S$	12	5411	1.08	0.16	4.072	1
$z^1P^o - f^1D$	21	5625	1.32	0.00	4.072	1
$z^1P^o - e^1P$	27	5695	1.43	−0.03	4.072	1

TABLE 1—*Continued*

Multiplet	S	$\bar{\lambda}$	$\overline{\log X_0'}$	$\bar{Y}$	$\bar{X}_{J'}$	No. of Lines
	Ni I, $3d^9 4p - 3d^9 6s$					
$z^3P^o - g^3D$	9	4290	0.35	0.51	3.642	1
$z^3F^o - g^3D$	21	4370	0.55	0.63	3.626	3
$z^1D^o - g^3D$	15	4430	0.40	0.60	3.704	4
$z^1F^o - g^1D$	7	4400	0.85	0.40	3.831	1
$z^1D^o - g^1D$	5	4481	0.70	0.75	3.881	1
	Zr I, $4d^3 5s - 4d^3 5p$					
$a^5F - y^5G^o$	45	4688	1.22	−0.93	0.727	1
	Zr II, $4d^3 - 4d^2 5p$					
$b^2F - x^2F^o$	40	4333	1.34	−0.83	2.399	1
$b^4P - z^4D^o$	336	4415	1.52	−0.04	1.208	7
$a^2H - z^2G^o$	660	4420	2.51	−1.53	1.502	2
$a^2G - z^2F^o$	337.5	4640	2.22	−1.06	0.987	2

tional material and reductions for each multiplet of each array. For each transition array the mean value of Y for each multiplet was plotted against the corresponding mean lower excitation potential, $\bar{X}_{J'}$. The value of the excitation temperature T was computed from the slope of the best straight line that could be drawn through the points, and the value of L was determined from the intercept on the Y-axis. Figure 2, *a* and *b*, show the plots for the arrays *Fe* I $3d^6 4s 4p - 3d^6 4s 5s$ and *Ti* I $3d^3 4s - 3d^3 4p$. Each dot represents a mean value of Y for a multiplet; the size of the dot is indicative of the number of lines in the multiplet. For each of these two arrays it was found desirable to perform a least-squares solution in order to fit the best straight line to the plotted points. The result for *Fe* I turns out to be

$$T = 4150^\circ \pm 50^\circ \text{ (P.E.)},$$

and for *Ti* I

$$T = 4350^\circ \pm 200^\circ \text{ (P.E.)}.$$

The results for each transition array are contained in Table 2. The weights assigned to the temperature determinations are proportional to the product of the number of lines and the range of excitation potential employed for each array. If we include, for the present, all of the material in Table 2, the weighted mean excitation temperature of the reversing layer turns out to be 4200°. If all the errors involved in the temperature calculation were purely observational, it would be correct to adopt the value of 4200° for the

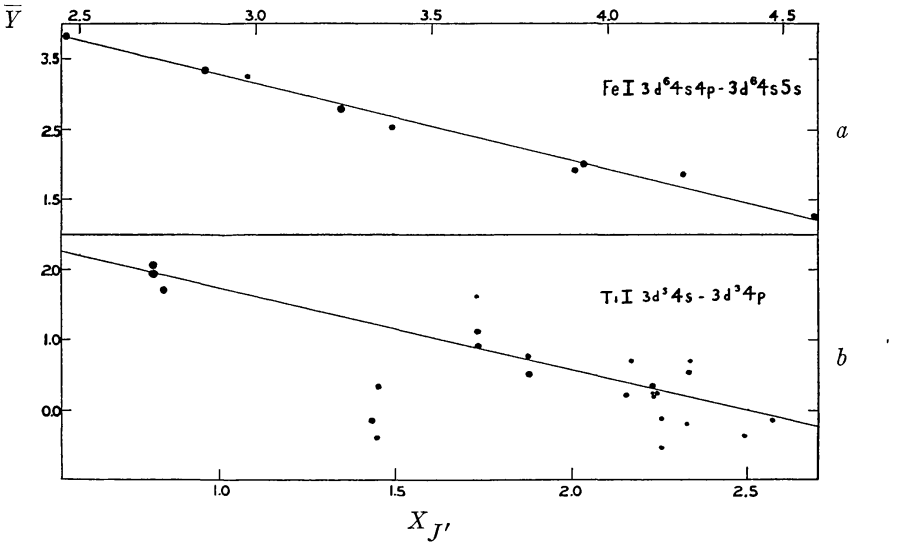

FIG. 2

mean temperature of the reversing layer. The departures of complex atoms from *LS* coupling and the existence of configuration interaction, however, produce errors in the calculation of theoretical multiplet strengths, which may be more serious than the observational errors. In order to facilitate the calculation of multiplet strengths on a large scale, it was necessary to assume that the electrons in an atom obey the rules of *LS* coupling and that individual configurations are isolated. *LS* coupling will occur when the spin-orbit interaction for a single electron is very small compared with the electrostatic interaction between electrons. This condition holds quite well for atoms of small nuclear charge. But as the nuclear charge increases, the spin-orbit interaction increases more rapidly than the

electrostatic interaction, and pronounced deviations from *LS* coupling occur. Certainly, for the atoms in the iron group, with which we have been chiefly concerned in the temperature determination, the assumption of *LS* coupling is no more than a first approximation. The most serious manifestation of departures from *LS* coupling is the overlapping of terms of different multiplicities and the consequent occurrence of intersystem combinations. The presence of

TABLE 2

Element	Transition Array	*T*	*L*	Weight
Ca I	$3d4s-3d4p$	1550	4.98	4
	$4s4p-4p^2$	2900	5.14	8
	$4s4p-4s4d$	2900	5.71	7
Ti I	$3d^34s-3d^34p$	4450	2.90	165
	$3d^24s4p-3d^24s5s$	2600	2.71	7
Ti II	$3d^3-3d^24p$	4800	2.51	28
V I	$3d^44s-3d^44p$	3850	2.19	46
Cr I	$3d^44s4p-3d^44s5s$	4150	4.56	20
Mn I	$3d^64s-3d^64p$	4850	5.21	26
	$3d^54s4p-3d^54s5s$	4350	5.43	14
Fe I	$3d^74s-3d^74p$	3650	6.19	17
	$3d^64s4p-3d^64s5s$	4150	6.47	167
Ni I	$3d^94p-3d^94d$	4800	4.78	16
	$3d^94p-3d^96s$	4450	4.74	2

intersystem lines in a spectrum usually implies that the strengths of permitted lines arising from the same lower levels are weaker than the simple theory indicates. The strengths of intersystem lines depend directly on the degree to which the levels of one term perturb the levels of another of differing multiplicity, and hence are a rough measure of the magnitude of departure from extreme *LS* coupling. In intermediate coupling there is no segregation of levels into terms, and all transitions obeying the *J*-selection rule are allowed.

It is significant that, while many intersystem lines are conspicuously strong in the spectra of iron-group atoms, they are considerably weaker, on the whole, than the permitted lines associated

with them. It appears reasonable to conclude, then, that of the two extreme types of coupling, *LS* and *jj*, the former is more nearly approximated by the atoms we are considering. It must be remembered, nevertheless, that *LS* coupling is no more than a first approximation to the true coupling, and that the multiplet strengths calculated on this basis will necessarily exhibit a considerable degree of scatter. In our determination of the solar temperature, however, the scatter will not be too serious a factor, provided a large number of lines varying widely in excitation potential are utilized. If, on the other hand, the calculated multiplet strengths are systematically too large as the excitation potential for the levels of the lower configuration increases, the negative slope of the $5040/T$ line will be too large, and the computed temperature will be too low. Another source of error in the calculation of multiplet strengths arises from the assumption that the configurations of a transition array are well isolated and are unperturbed by neighboring configurations. Actually, such isolation is rare in complex atoms, particularly with regard to the configurations $3d^k4p$ and $3d^{k-1}4s4p$ among atoms of the iron group. Because of the close proximity in the energies of the 3d and 4s electrons, the two configurations overlap and perturb each other to a large extent, with the result that each of the two configurations impresses its radiative characteristics on the other, and in so far as the ordinary selection rules are concerned, the configurations are indistinguishable from each other.

The existence of configuration interaction and of departures from *LS* coupling raises a question as to the reliability of the multiplet strengths utilized in the determination of the reversing-layer temperature. Fortunately, we have a means of checking our temperature calculation through the use of the *J*-file sum rule, which is valid for any coupling and is hence admirably suited to the problem. All the lines of a transition array which originate in (or terminate on) a given level constitute the *J*-file referring to that level—the sum of the strengths of these lines is the strength of the file. The *J*-file sum rule, which was first proved by Shortley, may be stated as follows:[10]

For any coupling, the strengths of the *J*-files referring to the levels

[10] Condon and Shortley, *Theory of Atomic Spectra*, p. 279.

of the initial/final configuration are proportional to $2J + 1$, provided that the jumping electron is not equivalent to any other in the final/initial configuration. In this statement the jumping electron may be equivalent to others in the initial/final configuration. In case it is not equivalent to others in *either* configuration, the sum rule holds for the files referring to *both* configurations. If the quantum numbers of the jumping electron are nl in configuration α and $n'l'$ in configuration β, the actual value of the strength of a file referring to a level of configuration α is

$$k(2J + 1)(l + 1)(2l + 3) \cdot \sigma^2 , \tag{7}$$

if $l' = l + 1$, and

$$k(2J + 1)(2l - 1)l \cdot \sigma^2 , \tag{8}$$

if $l' = l - 1$. Here k is the number of equivalent nl electrons in configuration α.

The determination of the solar temperature by means of the sum rule proceeds in a manner similar to that outlined above, except that the quantity X_0 is replaced by $\sum X_0$, where the summation is taken over the complete set of lines originating from a given lower J-level of the transition array, and the theoretical strength is replaced by the proper J-sum, which we denote by $\sum J$. An excellent feature of the sum-rule method is that it takes account of intersystem and interlimit combinations in the sums from the lower levels. In addition, when a near-by configuration perturbs the upper configuration of a transition array, we include in the sum all the lines from a given lower level to the levels of both upper configurations.[11] The sum-rule method thus takes into account completely both the departures from LS coupling and the influence of near-by configurations. Unfortunately, the application of the method requires the observation of complete sets of lines arising from the lower levels of an atom. For most atoms the material is not available, since many of the lines in a given set occur to the violet of λ 4036, the ultraviolet limit of Allen's measures. The lines of *Ti* I that arise from the configuration $3d^3 4s$ are nearly all available, however, and we have means of

[11] *Ibid.*, p. 281.

checking our previous temperature determination for *Ti* I. The most important transitions from the configuration $3d^34s$ are those to the configurations $3d^34p$ and $3d^24s4p$. The latter two configurations overlap each other and were therefore regarded as a single extended configuration in the calculation. Then, by (7) and (8), the sum of the strengths of all the lines originating from a level J of the configuration $3d^34s$ is equal to

$$\left.\begin{aligned} &3(2J+1)\phi_{4s-4p} + 18(2J+1)\phi_{3d-4p} \\ &\quad = 3(2J+1)(\phi_{4s-4p} + 6\phi_{3d-4p}) , \end{aligned}\right\} \tag{9}$$

and

$$\sum J = 3(2J+1) .$$

Table 3 lists the levels of $3d^34s$ that were available, the numbers of lines entering into the sum from each level, $\log \sum X_0$ for each set of lines and the corresponding value of $\log \sum J$, $\log \sum X_0/\sum J$, and the excitation potential $\chi_{J'}$ of each lower level. In Figure 3, $\log \sum X_0/\sum J$ is plotted against $\chi_{J'}$. The slope of the resulting straight line was computed by least squares and yields a value of $4400° \pm 100°$. The result agrees closely with the value of $4350°$ obtained by the use of individual line strengths. It is interesting to compare Figures 2 and 3 in connection with the qualitative theory of departures from *LS* coupling and of configuration interaction. The small amount of scatter in Figure 3 is conspicuous; what little there is can be ascribed to the presence of blends and to the observational errors. The behavior of the lines arising from the b^3F term provides a striking illustration of the effects of configuration interaction on the calculation of theoretical multiplet strengths. In Figure 2 the points corresponding to these lines fall far below the straight line. A glance at the *Ti* I term spectrum readily provides the explanation. The triad of terms y^3G^o, x^3F^o, and w^3D^o, of the configuration $3d^34p$, which combine with b^3F, are perturbed by neighboring terms of $3d^24s4p$, with the result that the lines of $3d^34s - 3d^34p$ are unduly weakened. When the transitions to the neighboring terms are included by means of the sum rule, the b^3F points are brought into much closer agreement with the others.

In adopting, for purposes of discussion, the best value of the temperature of the solar reversing layer, we need consider only the values derived from the lines of *Fe* I $3d^6 4s4p - 3d^6 4s5s$ (4150°),

TABLE 3

Term	J	No. of Lines	$1 + \log \Sigma X_0$	$\log \Sigma J$	$1 + \log \frac{\Sigma X_0}{\Sigma J}$	$X_{J'}$
a^5F.....	5	9	3.37	1.52	1.85	0.85
	4	12	3.30	1.43	1.87	0.83
	3	15	3.23	1.32	1.91	0.82
	2	10	3.22	1.18	2.04	0.82
	1	8	2.95	0.95	2.00	0.81
b^3F.....	4	12	2.51	1.43	1.08	1.45
	3	13	2.43	1.32	1.11	1.44
	2	10	2.30	1.18	1.12	1.42
a^5P.....	3	6	2.38	1.32	1.06	1.74
	2	7	2.16	1.18	0.98	1.73
	1	6	1.92	0.95	0.98	1.73
a^3G.....	5	10	2.28	1.52	0.76	1.88
	4	12	2.22	1.43	0.79	1.87
	3	8	2.05	1.32	0.73	1.87
a^3H.....	6	4	1.96	1.59	0.37	2.25
	5	3	1.83	1.52	0.31	2.24
	4	5	1.60	1.43	0.17	2.23
b^1G.....	4	5	1.68	1.43	0.25	2.26

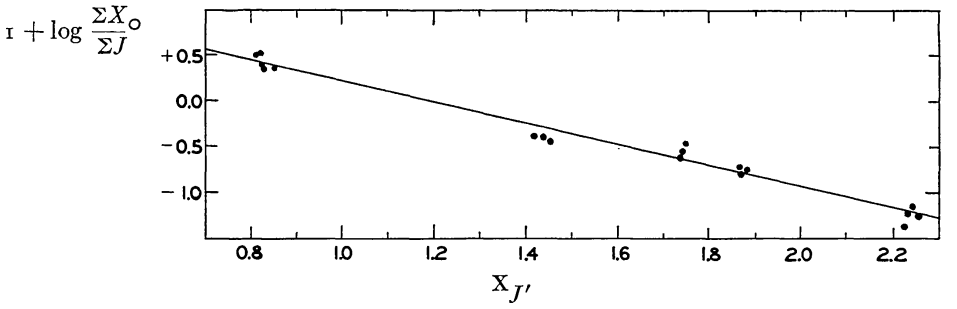

FIG. 3

Ti I $3d^3 4s - 3d^3 4p$ (4350°), and the value of 4400° calculated from the *Ti* I lines with the aid of the sum rule. All of the other determinations are of low weight and are of little significance. Since the

sum-rule method allows for all of the errors inherent in the calculation of multiplet strengths, we have chosen 4400° as the value best representing the mean effective excitation temperature of the solar reversing layer. There is still the possibility, however, that the difference between the *Fe* and *Ti* temperatures is real and that it indicates the presence of a temperature gradient in the reversing layer. If a pressure gradient exists in the solar atmosphere, the lines of easily ionized elements should arise from lower levels in the atmosphere than do the lines of elements that are more difficult to ionize. *Fe* I has an ionization potential of 7.8 volts, as compared with 6.8 volts for *Ti* I.

The temperature of 4400° is apparently inconsistent with the value of 5740° adopted in fitting the observations to the theoretical curve of growth. The lower value, however, is an excitation temperature, the higher one a kinetic temperature, and the two need not necessarily be the same. Furthermore, the method of computing the excitation temperature requires only an approximate knowledge of the kinetic temperature. A small error in v will produce an error only in the Doppler portion of the curve of growth, for, in the straight-line portions of the curve, v/c enters as a constant factor.

In the foregoing discussion we have assumed N_a to be constant with wave length. What effect will a variable opacity have on the determination of the reversing-layer temperature? If the general opacity of the solar atmosphere varies with wave length, N_a will exhibit a reciprocal variation. In an attempt to evaluate the opacity law we have assumed various temperatures and have determined the values of L for each multiplet. Since $\log N_a$ differs from L by an additive constant, we may examine the data for an opacity variation by plotting L against λ for each array and by noting the scatter in the observational points. If there is no systematic relation between the lower potential and the wave length, the scatter will obviously be a minimum for the temperature originally determined from the $5040/T$ diagram. Figure 4 shows the relation between excitation potential and wave length for the multiplets of *Ti* I $3d^3 4s - 3d^3 4p$ and for those of *Fe* I $3d^6 4s 4p - 3d^6 4s 5s$. It is quite obvious that the correlation is absent for the *Ti* I multiplets, but the mean lower excitation potentials of the *Fe* I multiplets show a progressive

increase with wave length. We should expect, therefore, that the law of opacity determined by equation (6) from the *Ti* I lines is independent of the temperature chosen. This expectation is verified when we plot the mean value of L for each multiplet against the corresponding mean wave length, with temperatures of 4500°, 5000°, and 5600° (Fig. 5). The three curves are very nearly parallel, but the scatter is slightly less for $T = 4500°$ than for either of the other two curves. Since, for the *Fe* I multiplets the mean lower ex-

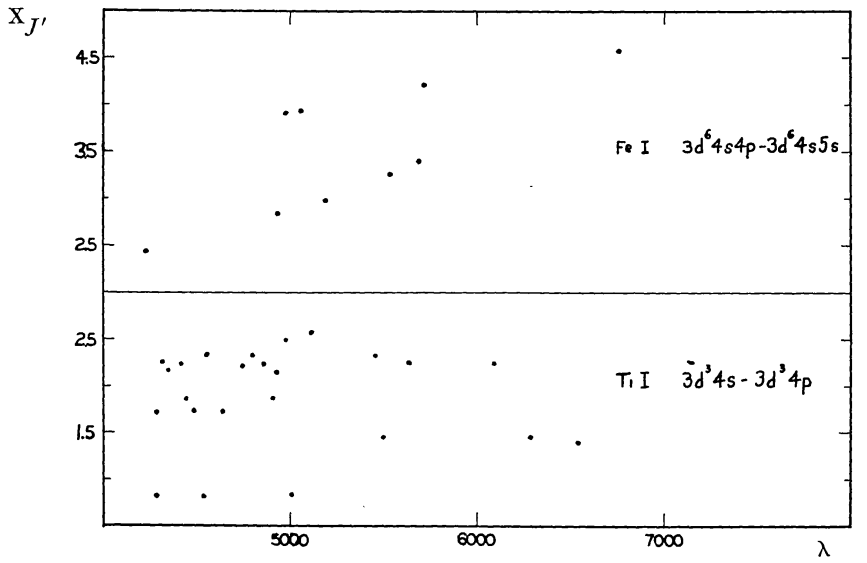

FIG. 4

citation potentials increase systematically with the wave length, the law of opacity determined from these multiplets by (6) should depend on the value of the temperature assumed. In Figure 6*a*, we have plotted the mean L's for the *Fe* multiplets against the mean wave lengths for a number of values of the temperature. The opacity law is seen to change conspicuously with the temperature. It is reasonable to assume, however, that the best value of the temperature to choose is that for which the scatter in the $L - \lambda$ diagram is a minimum. When we compute the sum of the squares of the residuals from the best straight line that can be drawn through each set of points, and plot the sums against the temperature, we find a sharp minimum at $T = 4100°$ (Fig. 6*b*). The resulting opacity

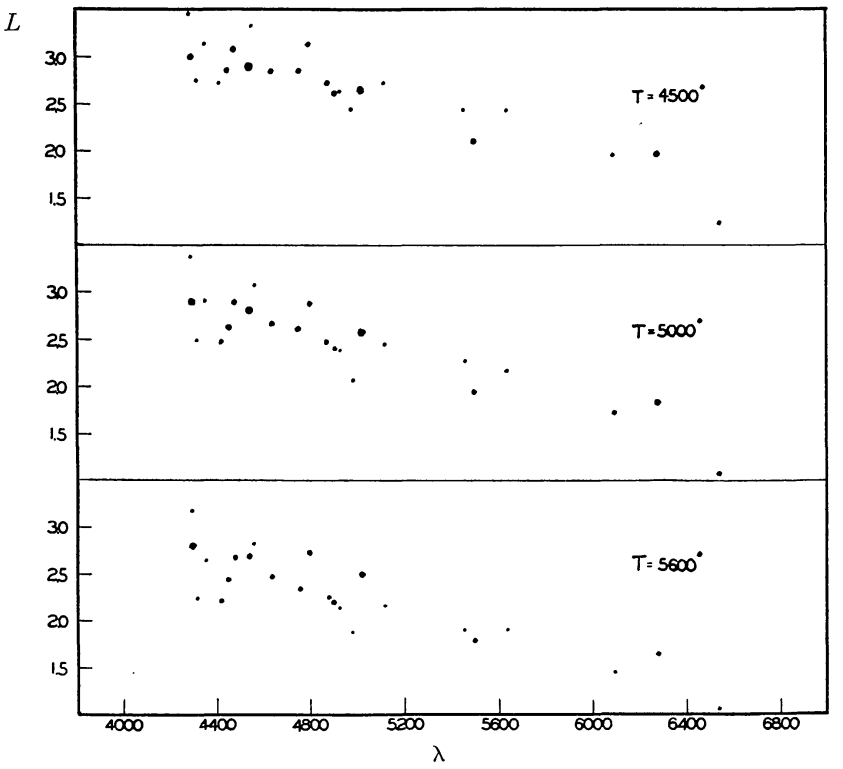

FIG. 5

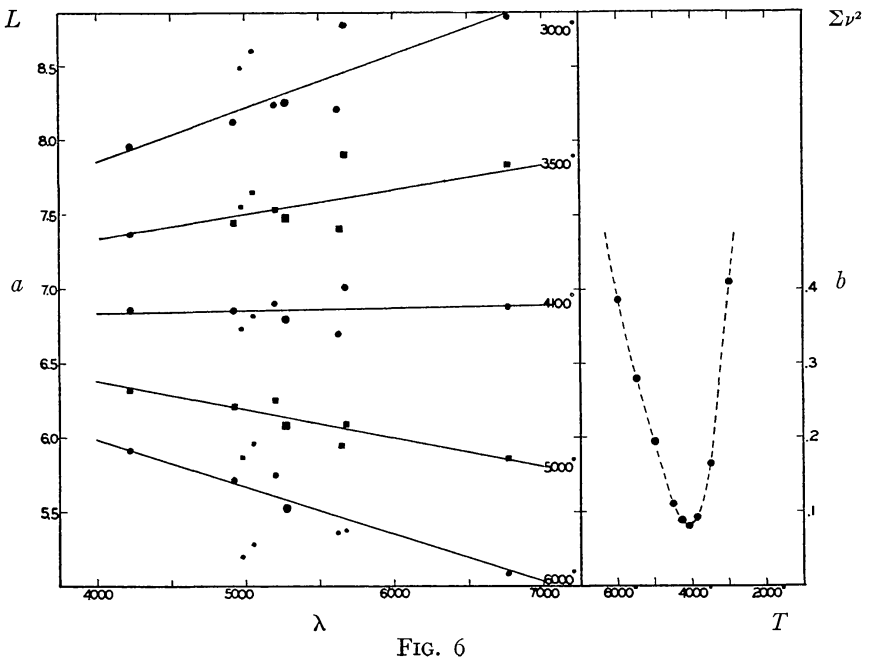

FIG. 6

law appears to be sensibly constant with λ. The scatter for *Ti* is considerable. The best line that can be drawn to represent the observations is controlled almost completely by the three points arising from the term b^3F. We have already pointed out that the theoretical strengths for these multiplets are probably too large. The points are to be raised by an indeterminable amount. The final opacity law for *Ti* will probably not be inconsistent with the λ^3 relation.

The difference between the opacity laws thus derived for *Ti* and *Fe* remains unexplained. According to Menzel and Pekeris,[12]

$$\left.\begin{aligned} L &= \text{Const.} - 3 \log \lambda - \log \left(e^{hc/\lambda KT} - 1\right) \\ &= \text{Const.} - 3 \log \lambda - \frac{1.2 \times 10^{-4}}{\lambda}, \end{aligned}\right\} \qquad (10)$$

for a homogeneous atmosphere (λ in centimeters, and $T = 5000°$). The foregoing expression predicts an increase of L with the increasing wave length, exactly the reverse of the observational results just obtained.

It should be remembered, however, that the theoretical opacity law was obtained on the assumption of a continuously varying quantum defect, to represent the effect of overlapping of successive series limits of the atoms undergoing ionization. The formula probably represents an upper limit for the opacity. The effect of all series limits to the red of a given wave length λ_0 is represented by the formula

$$L = \text{Const.} - 3 \log \lambda - \log \left(e^{hc/\lambda_0 KT} - 1\right). \qquad (11)$$

The relation between L and λ is very sensitive to the distribution of the neglected continua, and perhaps a constant opacity is not seriously in disagreement with theory. The λ^3 opacity law so frequently employed by investigators is seen to have a possible theoretical justification, though it does omit from consideration all continua originating in the visible spectral range.

The quantity L depends only on the product of N_a, the total number of atoms of a given element in a given stage of ionization above 1 square centimeter of the photosphere, and ϕ, the radial quan-

[12] *M.N.*, **96**, 77, 1935; cf. also Menzel, *loc. cit.*

tum integral for a transition array. If the relative ϕ's for different atoms are determined from quantum-mechanical calculations, the relative abundances of the elements may be computed. When the absolute values of the ϕ's are known, it will be possible to determine the absolute abundance of any element in a given stage of ionization. A quantitative study of abundances in the solar reversing layer, based on the foregoing considerations, is now in progress at the Harvard Observatory.

The unexpectedly low temperature here derived is not without precedent. In 1922, R. T. Birge,[13] who analyzed the solar *CN* bands by a method consistent with the one employed here, derived a solar temperature of $4300° \pm 500°$. Later band-spectrum analyses by Richardson[14] gave somewhat higher values but much greater probable errors. The temperature here determined is an effective excitation temperature. Any departures of the partition from thermodynamic equilibrium will be included in the result. The straightness of the line in Figure 3 indicates that such departures are small. The energy most effective for exciting atoms is that close to the center of the already existing Fraunhofer line. Consequently, the excitation temperature deduced might be expected to approach that of a black body emitting, not with photospheric intensity, but with an intensity corresponding to the emission in the line centers.[15] The low excitation temperature may be related to the known deficiency of solar radiation in wave lengths 4000–3000 A. Coblentz and Stair[16] have recorded an effective temperature of 4000°, as deduced from the gradient of intensity in the region 3400–2900 A.

It is a pleasure to record our appreciation to Dr. G. H. Shortley for his useful suggestions and comment on the solar temperature determination.

HARVARD OBSERVATORY
October 1937

DEFINITIONS OF ALGEBRAIC NOTATION

W	Equivalent width in IA
λ	Wave length
ν	Frequency

[13] *Ap. J.*, **55**, 273, 1922.
[14] *Ibid.*, **73**, 216, 1931.
[15] Cf. suggestion by Stewart, *M.N.*, **85**, 732, 1935.
[16] *Nat. Bur. Stand. Research Paper RP 899*, 1936.

ν	Root-mean-square kinetic velocity
Γ	Damping factor
f	Oscillator strength
$A(J, J')$	Einstein A
$s/\Sigma s$	Theoretical strength of a line in terms of the summed strength for the multiplet
S	Theoretical strength of a multiplet in a transition array in units of σ^2
σ^2	The square of the first-order radial component of electric moment for the given array
a_0	The radius of the first Bohr orbit
ϵ	Electronic charge
ϕ	$\sigma^2/a_0^2\epsilon^2$, i.e., σ^2 in atomic units
T	Temperature
N_a	The total number of atoms, per square centimeter column, of a given element in a given stage of ionization
$X_{J'}$	Excitation potential
$b(T)$	Partition function
μ	Molecular weight
R	Rydberg constant

NOTE ADDED IN PROOF

Our attention has been directed to a letter in *Nature*, **113**, 338, 1924 (cf. also *M.N.*, **85**, 732, 1925), by J. Q. Stewart, in which he points out that the conventional Schwarzschild value of 0.85 of the photospheric temperature for the temperature of a stellar reversing layer is subject to question, since in view of the small observed central intensities of absorption lines a stellar atmosphere may by no means be considered as a gray body. Stewart shows that the conventional temperature of 5100° for the solar reversing layer leads to a central intensity of 0.50 for the sodium D lines, and that a temperature of about 4000° is required by the Planck formula to reduce the central intensity to the observed value of 0.10. He suggests that an average temperature of about 0.7, that of the photospheric temperature, should be adopted for stellar reversing-layer temperatures.